Wang et al., Clin Med Biochemistry 2016, 2:1
DOI: 10.4172/2471-2663.1000110

Clinical & Medical Biochemistry

Research Article Open Access

One Computation Method of the Constant K_3/K_4 in Three-Compartment Modeling of ^{13}N-NH_3 PET Images Tractor

Zhenyou Wang*, Xueling Huang and Changxiu Song

Faculty of Applied Mathematics, Guangdong University of Technology, Guangzhou, PR China

Abstract

This study aims to quantitatively analyze and compute the velocity constant of three-compartment modeling, which is based on ^{13}N-NH_3 PET images of human brain tumors. We selected the parietal lobe, cerebellum, frontal lobe, and the average of these three reference regions to analyze the transfer constant ratio, K_3/K_4, in three-compartment modeling. The study was based on the results of three-compartment modeling. Data sampling was performed for a left frontal lobe tumor, and simultaneously, data sampling was performed for three reference regions (including the parietal lobe, cerebellum, and right frontal lobe). The dynamic frames were 4 × 10 s, 7 × 20 s, 4 × 60 s, and 1 × 480 s. The parietal lobe, cerebellum, frontal lobe and the average of the three reference regions, as determined by the slopes of the fitted curves, are 1.6207, 1.5931, 1.5293, and 1.5803, respectively. The F-test values are 5552.4, 2943.6, 3756.8, and 5650.2, respectively; the average F-test value is the largest. And we have experiment with 11 ROIs with REF in this way, they are the line relative. All the R^2 and P for all the fitted curves are almost 1, and all the P of all the fitted curves are almost 0. Moreover, the 95% confidence interval, which is based on the variance test, are enough short respectively. The comparison results show that the deviation and relative deviation for mean of REF are within the acceptable level. Thus, we have thought the K_3/K_4 as 0.5803; therefore, the transfer constant K_4 is about 1.72 times that of K_3 for the clinical use of ^{13}N-NH_3 PET tracer for brain tumors. The ^{13}N-NH_3 PET tracer is feasible for clinical use with brain tumors. The transfer constant, K_4, is approximately two times of K_3 in the three-compartment modeling of the parietal lobe, cerebellum, frontal lobe and the average of the three reference regions. This method is feasible and effective.

Keywords: Quantitative analysis; ^{13}N-NH_3 PET image; K_3/K_4; Reference region; Brain tumors

Introduction

Positron emission tomography (PET) is a medical imaging technique that is used to study tissue functions *in vivo* by a tracer, which is labeled with positron-emitting radionuclides. Arterial sampling is considered to be the accuracy standard for obtaining the input functions. However, arterial sampling is invasive, laborious and sensitive to errors, and it has a minor risk of adverse effects [1]. In a previous study [2], a new method was developed that combine's partial volume correction (PVC) during reconstruction with a simple automatic procedure for extracting the IDIF from the internal carotid arteries.

No particular model structure is assumed, which can be an advantage in many cases because one model may not describe equally well all data sets from the same region of interest (ROI). It is assumed that the plasma concentrations of unchanged tracer are monitored following tracer injection. The requirement of plasma measurements can be eliminated in some cases when a reference region is available.

The kinetic modeling of data that are obtained from PET can provide quantitative information regarding the spatial distribution of radiopharmaceuticals [1]. This modeling often requires knowledge of the input function that is traditionally obtained by arterial sampling, which is a burdensome and potentially risky procedure. Image-based time activity curves, which are obtained by placing regions of interest (ROIs) over vascular structures on PET dynamic studies, are an appealing way to obtain individual input functions, concurrently reducing or obviating the requirement for blood samples.

For brain scans, several studies have demonstrated the possibility of obtaining a reliable input function using the smaller intracranial vessels, such as the internal carotids [2] or venous sinuses [3]. Positron emission tomography is widely used to investigate tumors in the brain [4].

Several PET tracers have been applied to the investigation of micro-vascular structures in proof of-principle experiments. Partial volume effects that are caused by overlapping signals from other tissues can be significant when the tumor size is less than twice the scanner resolution [5]. The measurement of the tumor blood volume can be achieved by the inhalation of ^{11}C-CO, which then forms ^{11}C-CO-hemoglobin. Unlike ^{15}O-H_2O, ^{11}C-CO-hemoglobin remains entirely intravascular and enables the calculation of blood volume from the ratio of tracer concentrations in tissue to that in blood [6].

^{13}N (half-life: 9.965 min, 100% decay) is one of the most important of all positron emitters and has been primarily used in nuclear medicine in the chemical form ^{13}N-NH_3 [7] or as enzymatically synthesized ^{13}N-labeled amino acids [8]. Cardiac ^{13}N-ammonia (^{13}N-NH_3) PET is frequently used to assess myocardial blood flow and the coronary flow reserve [9]. However, gated cardiac ^{13}N-NH_3 imaging is not currently used for the estimation of left ventricular function or for brain tumors. In addition, in clinical applications, ^{13}N is of limited use compared with other positron emitters, such as ^{11}C and ^{18}F, which is primarily due to its short half-life of 10 minutes. However, the short half-life is also convenient to both shorten the time in the clinic and to shorten the pain of the patient [10]. ^{13}N may come to be used more widely if more ^{13}N-labeled compounds are made available. High specific activity may also increase the applicability of ^{13}N-labeled compounds for receptor studies using PET [11].

In this paper, we analyzed kinetic modeling that uses the ^{13}N-NH_3 PET tracer for brain tumors in a clinically used reference region method. Because the parietal lobe, cerebellum and right frontal lobe have close ties with the tumor regions (left frontal lobe) of the brain,

***Corresponding authors:** Zhenyou Wang, Faculty of Applied Mathematics, Guangdong University of Technology, Guangzhou, 510520, PR China, E-mail: zhenyouw@gdut.edu.cn

Received December 09, 2015; **Accepted** January 05, 2016; **Published** January 12, 2016

Citation: Wang Z, Huang X, Song C (2016) One Computation Method of the Constant K_3/K_4 in Three-Compartment Modeling of ^{13}N-NH_3 PET Images Tractor. Clin Med Biochemistry 2: 110. doi:10.4172/2471-2663.1000110

whether structurally or functionally, we selected the three reference regions to compute the relative of the constant K_3/K_4 for three-compartment modeling. In addition, we analyzed and statistically tested for the transfer constant of the three-compartment modeling.

Materials and Methods

The institutional review board of our hospital approved this retrospective study. A 47-year-old man had been diagnosed with a brain tumor on the left frontal lobe, detailed information regarding the study purpose and imaging procedure were explained to the patient, and informed consents were obtained from the patient.

To perform the quantitative analysis of ^{13}N-NH_3 PET, we have used three-compartment modeling and have selected three reference regions (including the parietal lobe, cerebellum, and right frontal lobe) that are close to the tumor region (left frontal lobe). Based on the relation between the region of interest (ROI) and the region of reference (REF), we have computed the constant K_3/K_4 of the three-compartment modeling, which is based on the ^{13}N-NH_3 PET imaging of a human brain tumor.

PET imaging

Tracers were produced at our center by applying standard techniques and commercially available systems for isotope generation (Ion Beam Applications, Cyclone-10, Belgium). PET/CT imaging was performed with a Gemini GXL 16 scanner (Philips, Netherlands) in the 3-dimensional acquisition mode. The specific imaging protocol for brain was selected with a FOV of 180 mm, and the Trans axial spatial resolution was 2 mm full width at half maximum at the center of the FOV for ^{13}N-ammonia. PET images were reconstructed by the line-of-response RAMLA algorithm, with low-dose CT images for attenuation correction, which resulted in 3-dimensional images that consisted of $128 \times 128 \times 90$ voxels of $2.0 \times 2.0 \times 2.0$ mm^3.

Because the half-life of ^{13}N is 9.965 min, there is 100% decay [11]. For the patient, the tracers were examined with a time interval of at least 24 hours between the scans, and fasting for more than 8 hours was required before ^{13}N-ammonia imaging. At 5 minutes after the injection of ^{13}N-ammonia (370-740 MBq), a 15-minute PET acquisition began (Figure 1).

The study was based on the results of three-compartment modeling. We have obtained data sampling from a left frontal lobe tumor; simultaneously, we have obtained data from the three reference regions (including the parietal lobe, cerebellum, and right frontal lobe) and the average of the three reference regions. The dynamic frames consisted of 4×10 s, 7×20 s, 4×60 s, and 1×480 s.

Methods

For reversible systems, the form of the graphical analysis equation can be derived from the compartmental equations that describe tracer accumulation in tissue. For the two-tissue compartment model, the compartment ordinary differential equations are shown [1,2].

In the equations, Cp (t), C1 (t) and C2 (t) are concentrations for each compartment at time t. The units of concentrations that are used in the examples that are presented in this paper are Ci/mL. The transfer constants, K_1, K_2, K_3 and K_4, describe the tracer concentration efflux between tissue and plasma. K_1 describes the transfer from plasma to tissue and is a function of blood flow, capillary permeability, and plasma protein binding. K_2 describes the transfer from tissue to plasma and is a function of blood flow. K_3 and K_4 are, respectively, the product of a bimolecular rate constant and the concentration of free receptor/enzyme, which is assumed to be constant. However, in experiments with changing neurotransmitter levels, K_3 and K_4 represent an average over the duration of the experiment.

The transfer constant and the distribution volume ratio (DVR) can be calculated directly using the graphical method with data from a reference region [REF (t)] and with an average tissue-to-plasma efflux constant. In fact, the DVR changes when we use a different conference region and a different tracer. Specifically, the DVR that we calculated is a relative value; thus, DVR is calculated using the following equation:

$$|DVR-1|=k_3/k_4.$$

Results

^{13}N-NH_3 PET images were reconstructed. The reconstruction matrix was 128×128 pixels, with a 2 mm pixel size. We have obtained 1440 (16×90) images.

We have selected three reference regions (including the parietal lobe, cerebellum, and right frontal lobe) that are close to the tumor region (left frontal lobe) and the average gray value of the region. For fitting convenience, we have used the formulation y=bx+c, and the fitting results are shown in Table 1 (Figure 2).

Discussion

Single scan acquisitions in PET are the most commonly protocols that are used in clinical imaging, irrespective of the tracer or the organ to be imaged. However, the obtained single scan images are primarily used for qualitative observations only. In brain imaging with PET, when the input curve is not available, the simulation or reference images can be converted to parametric images, which can be archived. These reference images are also useful for patient follow-up, for database constitution, and particularly for quantitative diagnoses.

From Table 1, among the reference regions are the line relative. If the parietal lobe is the ROI, and we take the cerebellum, right frontal

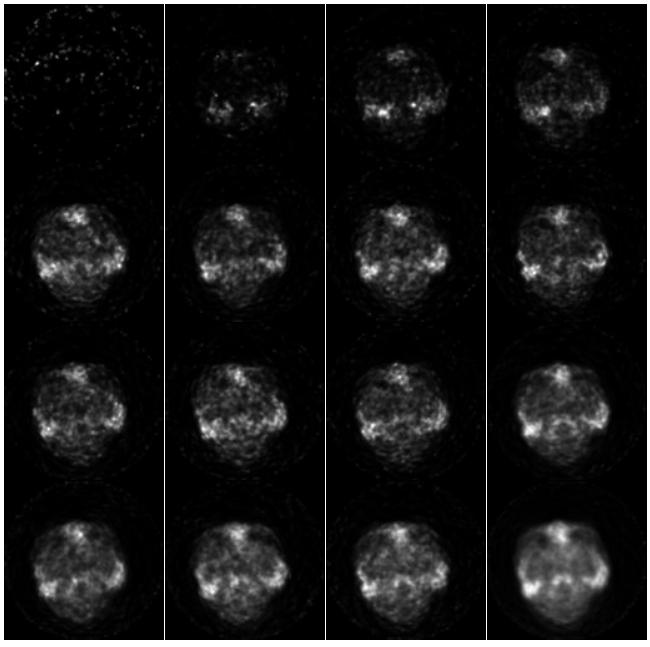

Figure 1: Sampling images of the tumor (10 s, 20 s, 30 s, 40 s, 60 s, 80 s, 100 s, 120 s, 140 s, 160 s, 180 s 240 s, 300 s, 360 s, 420 s, 900 s` images).

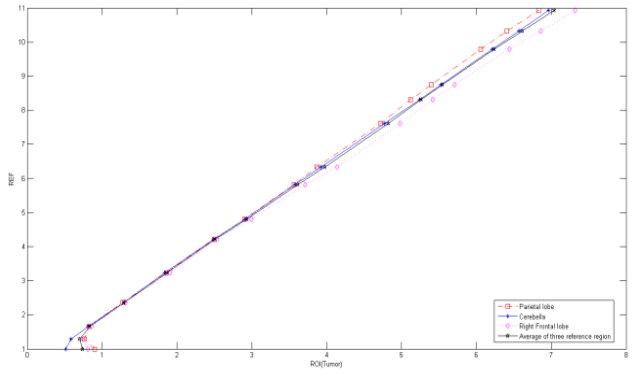

Figure 2: Fit curves of the ROI (tumor) and the REF.

lobe and the average of the three reference regions as the REF, then the calculated slopes of the fitted curves are 0.9827, 0.9436, and 0.9750, respectively. If the cerebellum is the ROI and we take the cerebellum, right frontal lobe and the average of the three reference regions as the REF, then the slopes of fitted curves are 1.0168, 0.9598, and 0.9918, respectively. If the right frontal lobe is the ROI and we take the cerebellum, right frontal lobe and the average of the three reference regions as the REF, then the slopes of the fitted curves are 1.0595, 1.0415, and 1.0332, respectively. The F-test values are 22417, 35993, 104140, 18802, 15069, 43701, 33389, 15097, and 59976. All the R^2 and P for all the fitted curves are almost 1, and all the P of all the fitted curves are almost 0. Therefore, this method is feasible and effective.

From Table 1, the reference region and the tumor region are relatively in line. In addition, the slopes of the fitted curves for the parietal lobe, cerebellum, right frontal lobe and the average of the three reference regions are 1.6207, 1.5931, 1.5293, and 1.5803, respectively. Thus, based on the method that is described in this paper, we can compute the relative constant K_3/K_4 of the three-compartment modeling, which are 0.6207, 0.5931, 0.5293, and 0.5803, respectively. Based on the computer data and the resulting analysis of the clinical use of PET ^{13}N-NH_3 tracer kinetic modeling of a brain tumor using the reference region method, we have found that the transfer constant K_4 of the modeling is approximately two times the transfer constant of K_3.

Moreover, the 95% confidence interval, which is based on the variance test, are [1.5943, 1.6471], [1.5644, 1.6218], [1.5006, 1.5580], and [1.5548, 1.6059], respectively. The confidence interval of the average is the shortest interval. The F-test values are 5552.4, 2943.6, 3756.8, and 5650.2, respectively, with the average of the regions being the largest value, i.e., the average is much more prevalent than the others are in the four results. Thus, we have chosen the K_3/K_4 value of 0.5803; therefore, the transfer constant K_4 is 1.7216 times the transfer constant K_3 for the clinical use of PET ^{13}N-NH_3 tracer for brain tumor imaging.

From Table 2, we have experiment with 11 ROIs with REF in this way, they are the line relative. All the R^2 and P for all the fitted curves are almost 1, and all the P of all the fitted curves are almost 0. Moreover, the 95% confidence interval, which is based on the variance test, are enough short respectively. The F-test values are meeting the requirement of the F-test table respectively. Thus, the transfer constant K_4 is about 1.7 times the transfer constant K_3 for the clinical use of PET ^{13}N-NH_3 tracer for brain tumor imaging. Therefore, this method is feasible and effective based on these results.

From Table 3, the mean value of K_4/K_3 is 1.6907 with cerebellum REF, and the variance is 0.0254. The mean value of K_4/K_3 is 1.8746 with frontal lobe REF, and the variance is 0.0405. The comparison results show that the deviation and relative deviation for mean of REF are within the acceptable level. From Table 4, The comparison results show that the deviations between this paper with method [12], method [13] and method [14] are within the acceptable level.

To avoid withdrawing blood samples from patients and handling radioactive samples, in this work, we proposed a new feasible and effective reference method to calculate parametric images for the analysis of ^{13}N-NH_3 tracer kinetic modeling. Additionally, we determined that the average of the last three conference regions (including the parietal lobe, cerebellum, and right frontal lobe) are optimal in the four results for the tumor (left frontal lobe). Therefore, this method is feasible and valid, with the average of the several related or associated regions being taken as the REF for the ROI.

ROI	REF	b	K_3/K_4	95% confidence interval	R^2	F	P
Tumor-1	Parietal lobe	1.6207	0.6207	[1.5943, 1.6471]	1.0e+003*0.0010	5552.4	0
Tumor-1	Cerebellum	1.5931	0.5931	[1.5644, 1.6218]	1.0e+004*0.0001	2943.6	0
Tumor-1	Frontal lobe	1.5293	0.5293	[1.5006, 1.5580]	1.0e+003*0.0010	3756.8	0
Tumor-1	Average	1.5803	0.5803	[1.5548, 1.6059]	1.0e+003*0.0010	5650.2	0
Parietal lobe	Cerebellum	0.9827	----	[0.9663, 0.9991]	1.0e+003*0.0010	22417	0
Parietal lobe	Frontal Lobe	0.9436	----	[0.9354, 0.9519]	1.0e+004*0.0001	35993	0
Parietal lobe	Average	0.975	----	[0.9672, 0.9829]	1.0e+003*0.0010	104140	0
Cerebellum	Parietal lobe	1.0168	----	[0.9998, 1.0337]	1.0e+003*0.0010	18802	0
Cerebellum	Frontal lobe	0.9598	----	[0.9488, 0.9708]	1.0e+004*0.0001	15069	0
Cerebellum	Average	0.9918	----	[0.9828, 1.0008]	1.0e+003*0.0010	43701	0
Frontal Lobe	Parietal lobe	1.0595	----	[1.0502, 1.0687]	1.0e+003*0.0010	33389	0
Frontal Lobe	Cerebellum	1.0415	----	[1.0295, 1.0534]	1.0e+004*0.0001	15097	0
Frontal Lobe	Average	1.0332	----	[1.0292, 1.0372]	1.0e+003*0.0010	59976	0

Table 1: Results of the tumor with parietal lobe, cerebellum and right frontal lobe.

ROI	REF	b	K_3/K_4	95% confidence interval	R^2	F	P
Tumor-1	Parietal lobe	1.6207	0.6207	[1.5943, 1.6471]	1.0e+003*0.0010	5552.4	0
Tumor-1	Cerebellum	1.5931	0.5931	[1.5644, 1.6218]	1.0e+004*0.0001	2943.6	0
Tumor-1	Frontal lobe	1.5293	0.5293	[1.5006, 1.5580]	1.0e+003*0.0010	3756.8	0
Tumor-1	Average	1.5803	0.5803	[1.5548, 1.6059]	1.0e+003*0.0010	5650.2	0
Tumor-2	Cerebellum	1.5801	0. 5801	[1.5775, 1.6151]	1.0e+003*0.0010	5252.6	0
Tumor-3	Cerebellum	1.5986	0.5986	[1.5884, 1.6235]	1.0e+003*0.0010	3128.6	0
Tumor-4	Cerebellum	1.5791	0. 5791	[1.5606, 1.6081]	1.0e+003*0.0010	3552.1	0
Tumor-5	Cerebellum	1.5913	0.5913	[1.5698, 1.6169]	1.0e+003*0.0010	3945.2	0
Tumor-6	Cerebellum	1.6002	0.6002	[1.5845, 1.6216]	1.0e+003*0.0010	2198.4	0
Tumor-7	Cerebellum	1.5988	0.5988	[1.5771, 1.6245]	1.0e+004*0.0001	2886.1	0
Tumor-8	Frontal lobe	1.5383	0.5383	[1.5108, 1.5625]	1.0e+004*0.0001	3056.7	0
Tumor-9	Frontal lobe	1.5468	0.5468	[1.5248, 1.5759]	1.0e+004*0.0001	3385.6	0
Tumor-10	Frontal lobe	1.5201	0.5201	[1.5083, 1.5569]	1.0e+003*0.0010	2983.8	0

Table 2: Results of the 10 tumor ROIs for REF.

ROI	REF	K_3/K_4	K_4/K_3	K4/K3 Mean of REF	Variance of K_4/K_3	Deviation FOR Mean of REF	Relative Deviation FOR Mean of REF
Tumor-1	Cerebellum	0.5931	1.6861	1.6907	0.0254	-0.0046	-0.28%
Tumor-2	Cerebellum	0.5801	1.7238			0.0331	1.92%
Tumor-3	Cerebellum	0.5986	1.6706			-0.0201	-1.21%
Tumor-4	Cerebellum	0.5791	1.7268			0.0361	2.09%
Tumor-5	Cerebellum	0.5913	1.6912			0.0005	0.03%
Tumor-6	Cerebellum	0.6002	1.6661			-0.0246	-1.48%
Tumor-7	Cerebellum	0.5988	1.6700			-0.0207	-1.24%
Tumor-1	Frontal lobe	0.5293	1.8893	1.8746	0.0405	0.0147	0.78%
Tumor-8	Frontal lobe	0.5383	1.8577			-0.0169	-0.91%
Tumor-9	Frontal lobe	0.5468	1.8288			-0.0458	-2.50%
Tumor-10	Frontal lobe	0.5201	1.9227			0.0481	2.50%

Table 3: Deviation analysis of the 10 tumor ROIs for REF.

ROI	REF	K_4/K_3	Method[12]	Deviation between this paper with method [12]	Method [13]	Deviation between this paper with method [13]	Method [14]	Deviation between this paper with method [14]
Tumor-1	Cerebellum	1.6861	1.6953	-0.0092	1.6788	0.0072	1.7187	-0.0327
Tumor-2	Cerebellum	1.7238	1.7084	0.0155	1.7226	0.0013	1.7490	-0.0252
Tumor-3	Cerebellum	1.6706	1.6604	0.0102	1.6613	0.0093	1.6816	-0.0110
Tumor-4	Cerebellum	1.7268	1.7209	0.0059	1.7250	0.0018	1.7440	-0.0172
Tumor-5	Cerebellum	1.6912	1.6753	0.0158	1.6986	-0.0074	1.7027	-0.0115
Tumor-6	Cerebellum	1.6661	1.6590	0.0071	1.6640	0.0021	1.6517	0.0145
Tumor-7	Cerebellum	1.6700	1.6742	-0.0042	1.6761	-0.0061	1.7035	-0.0335
Tumor-8	Frontal lobe	1.8577	1.8552	0.0025	1.8633	-0.0056	1.8745	-0.0168
Tumor-9	Frontal lobe	1.8288	1.8168	0.0120	1.8277	0.0011	1.8678	-0.0390
Tumor-10	Frontal lobe	1.9227	1.9214	0.0013	1.9191	0.0036	1.9445	-0.0218

Table 4: Deviation analysis of the 10 tumor ROIs for REF.

Acknowledgements

We would like to thank the National Natural Science Foundation of China (No. 11401115, 11471012), the Project of Department of Education of Guangdong Province (No **13KJ0396**).

References

1. Lammertsma AA (2002) Radioligand studies: imaging and quantitative analysis. Eur Neuropsychopharmacol 12: 513-516.
2. van der Weerdt AP, Klein LJ, Boellaard R, Visser CA, Visser FC, et al. (2001) Image-derived input functions for determination of MRGlu in cardiac (18)F-FDG PET scans. J Nucl Med 42: 1622-1629.
3. Litton JE (1997) Input function in PET brain studies using MR-defined arteries. J Comput Assist Tomogr 21: 907-909.
4. Chen K, Bandy D, Reiman E, Huang SC, Lawson M, et al. (1998) Noninvasive quantification of the cerebra 18 metabolic rate for glucose using positron emission tomography, F-fluoro-2-deoxyglucose, the Patlak method, and an image-derived input function. J Cereb Blood Flow Metab 18: 716-723.
5. Wahl LM, Asselin MC, Nahmias C (1999) Regions of interest in the venous sinuses as input functions for quantitative PET. J Nucl Med 40: 1666-1675.
6. Chen W, Silverman DH (2008) Advances in evaluation of primary brain tumors. Semin Nucl Med 38: 240-250.
7. Bacharach SL, Libutti SK, Carrasquillo JA (2000) Measuring tumor blood flow with H(2)(15)O: practical considerations. Nucl Med Biol 27: 671-676.
8. Phelps ME, Huang SC, Hoffman EJ, Kuhl DE (1979) Validation of tomographic measurement of cerebral blood volume with C-11-labeled carboxyhemoglobin. J Nucl Med 20: 328-334.
9. Khorsand A, Graf S, Eidherr H, Wadsak W, Kletter K, et al. (2005) Gated cardiac 13N-NH3 PET for assessment of left ventricular volumes, mass, and

ejection fraction: comparison with electrocardiography-gated 18F-FDG PET. J Nucl Med 46: 2009-2013.

10. Cooper AL, Sheu KF, Blass JP (1996) Normal gluta- mate metabolism in Alzheimer's disease fibroblasts deficient in alpha-ketoglutarate dehydrogenase complex activity. Develop Neurosci 18: 499-504.

11. Shi X, Zhang X, Yi C, Wang X, Chen Z, et al. (2013) The combination of 13N-ammonia and 18F-FDG in predicting primary central nervous system lymphomas in immunocompetent patients. Clin Nucl Med 38: 98-102.

12. Hori Y, Ihara N, Teramoto N, et al. (2015) Noninvasive quantification of cerebral metabolic rate for glucose in rats using (18)F-FDG PET and standard input function. J Cereb Blood Flow Metab 35: 1664-1670.

13. Juhász C, Dwivedi S, Kamson DO, Michelhaugh SK, Mittal S (2014) Comparison of Amino Acid Positron Emission Tomographic Radiotracers for Molecular Imaging of Primary and Metastatic Brain Tumors. Mol Imaging 13: 2310/7290.2014.00015.

14. Li F, Joergensen JT, Hansen AE, Kjaer A (2014) Kinetic modeling in PET imaging of hypoxia. Am J Nucl Med Mol Imaging 4: 490-506.

Citation: Wang Z, Huang X, Song C (2016) One Computation Method of the Constant K_3/K_4 in Three-Compartment Modeling of ^{13}N-NH_3 PET Images Tractor. Clin Med Biochemistry 2: 110. doi:10.4172/2471-2663.1000110